Optimal State-Space Control of a Gas Turbine Engine

J. W. Watts

T. E. Dwan

C. G. Brockus

Weapons and Systems
Engineering Department,
U.S. Naval Academy,
Annapolis, MD 21402

An analog fuel control for a gas turbine engine was compared with several state-space derived fuel controls. A single-spool, simple cycle gas turbine engine was modeled using ACSL (high level simulation language based on FORTRAN). The model included an analog fuel control representative of existing commercial fuel controls. The ACSL model was stripped of nonessential states to produce an eight-state linear state-space model of the engine. The A, B, and C matrices, derived from rated operating conditions, were used to obtain feedback control gains by the following methods: (1) state feedback; (2) LQR theory; (3) Bellman method; and (4) polygonal search. An off-load transient followed by an on-load transient was run for each of these fuel controls. The transient curves obtained were used to compare the state-space fuel controls with the analog fuel control. The state-space fuel controls did better than the analog control.

1.0 Introduction and Model Description

The development of a state-space fuel control on a single-shaft, simple cycle gas turbine engine is the subject of this paper. A model of this simple engine with analog fuel control was available. The load transients of this model have been compared with actual load transients and found to be accurate. This verified model becomes a tool for developing multimode state-space controllers for more complicated engines. For example, a possible future high-efficiency engine for powering naval ships is an intercooled, regenerated (ICR) gas turbine engine [1]. The control for this future engine will involve monitoring several outputs and will have three to five inputs. The number of inputs will vary with the mode of operation. A computer in the control loop will allow for many sophisticated modes and, also, allow for improvements in control strategy after initial development and even after installation. Fuel controls for future engines will be developed and verified with this simpler engine model as a tool.

A simple cycle single-shaft gas turbine engine was modeled using ACSL (Advanced Continuous Simulation Language) [2]. Figure 1 shows the engine components and the three control volumes used for modeling the dynamic behavior. For each control volume a mass balance and an energy balance produced two first-order differential equations [3]. For example, the compressor control volume V3 equations are:

Mass balance:

$$DW3 = WA2 - WA3 - WBL \qquad (1.1)$$

where:

DW3 is change in mass in V3 per unit time

WA2 is mass rate into V3

WA3 is mass rate out of V3

WBL is all bleed flow rates from V3

Energy balance:

$$DT3 = ((WA2*(H3P - H3))/CV3 + T3*DW3*(GM3 - 1)/W3 \qquad (1.2)$$

where:

DT3 is the time derivative of exit temperature

H3 is enthalpy at exit of V3 without considering the volume storage of V3

H3P is enthalpy at exit considering storage

CV3 is the heat capacity (const. vol.) at exit

T3 is the temperature at the exit of V3

GM3 is the ratio of the heat capacities at the exit

W3 is the mass in the control volume V3

There are three control volumes in this model. A mass balance and an energy balance on each one yields six first-order dif-

Fig. 1 Engine components and control volumes
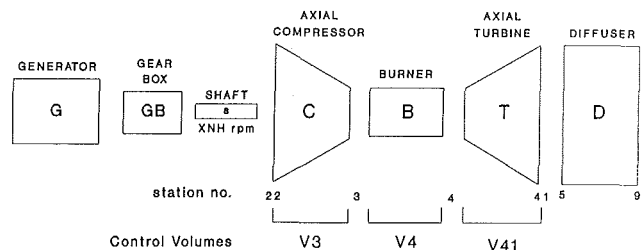
V3 = flow spaces of compressor

V4 = flow spaces of burner

V41 = flow spaces of turbine

ferential equations of the type shown above. A seventh differential equation is needed to define an energy balance on the rotating group. A torque imbalance (torque input from the turbine and torque output to the compressor and to the load) will produce an acceleration of the rotating group.

In addition the model has sensor delays, actuator delays, and lead-lag elements in the fuel control. A total of 11 states are present in the unaltered model. For purposes of devising a state-space fuel control, the number of states is reduced to eight. These are the control volume states and the shaft speed for a total of seven states. It is convenient to add an eighth state, integral of speed, so that the error in speed can be driven to zero. A ninth state, derivative of speed, provides anticipatory control at the expense of being sensitive to noise. This ninth state was obtained from the eight-state model by taking the dot product of the first row of the A matrix with the state vector. Only the polygonal search method used a control gain on this ninth state. The states in the state-space model are:

1 WGG shaft speed, rad/s
2 WGGINT integral of WGG, rad
3 T41 exit temperature from the turbine, R
4 W41 mass in the turbine control volume, lb
5 T4 inlet temperature to the turbine, R
6 W4 mass in the burner control volume, lb
7 T3 exit temperature from the compressor, R
8 W3 mass in the compressor control volume, lb
9 DWGG shaft acceleration, rad/s^2

The state-space fuel control gains (up to nine in number) were gains on each of these nine states.

2.0 Analysis

A good introduction to state-space methods and optimal control can be found in numerous texts, for example, Phillips and Harbor [4]. A fundamental knowledge of state-space methods is assumed in the rest of this development. With the analog model resident in ACSL, it is possible through ACTION and PROCED statements to look at various load set points and obtain perturbation models of the form [4]:

$$\delta \dot{\mathbf{x}} = A \delta \mathbf{x} + B \delta \mathbf{u} \tag{2.1}$$

where the A matrix is $(n \times n)$ and is the standard Jacobian array of the form

$$A = \begin{bmatrix} \dfrac{\partial f_1}{\partial x_1} & \dfrac{\partial f_1}{\partial x_2} & \cdots \\ \vdots & & \\ \dfrac{\partial f_n}{\partial x_1} & \cdots & \dfrac{\partial f_n}{\partial x_n} \end{bmatrix}_{x^0, u^0} \tag{2.2}$$

and

$$B = \begin{bmatrix} \dfrac{\partial f_1}{\partial u_1} & \dfrac{\partial f_1}{\partial u_2} & \cdots \\ \vdots & & \\ \dfrac{\partial f_n}{\partial u_1} & \cdots & \dfrac{\partial f_n}{\partial u_m} \end{bmatrix}_{x^0, u^0} \tag{2.3}$$

and the dimension of B is $(n \times m)$. The $\mathbf{x}^0$ and $\mathbf{u}^0$ vectors represent the selected operating point nominal values where

$$\mathbf{x} = \mathbf{x}^0 + \delta \mathbf{x} \tag{2.4}$$

and

$$\mathbf{u} = \mathbf{u}^0 + \delta \mathbf{u} \tag{2.5}$$

The output matrix, C, is also available and matrix D is null for these models. Varying the load, several operating points were established. The A, B, and C arrays were identified at

each of these operating points using the ASCL JACOB command and routed directly into MATLAB [5], a high-level programming tool available for systems analysis.

2.1 Scaling. The A matrices identified using this Jacobian procedure are, of course, very poorly conditioned arrays. Following Brockus [6], for a set of state equations given in the form

$$\dot{\mathbf{x}} = A \mathbf{x} + B \mathbf{u} \tag{2.6}$$

Let the normalizing constant (scale factor) for variable x_i be denoted X_i, and let the scaled variable z be related to the state variables by the linear transformation

$$\mathbf{x} = T \mathbf{z} \text{ in which } x_i = X_i z_i \tag{2.7}$$

The T matrix so defined is diagonal with the scale factors constituting the diagonal elements. Its inverse is equally simple, being diagonal with the inverse scale factors on the diagonal. Thus the completed transform

$$\dot{\mathbf{x}} = T^{-1} A T \mathbf{z} + T^{-1} B u$$

or

$$\mathbf{z} = A_s \mathbf{z} + B_s u \tag{2.8}$$

is a very simple one in which it is apparent that the scaled A matrix is formed by dividing row i of the system matrix by scale factor i, and by multiplying column j of the system matrix by scale factor j. Therefore if

$$A = [a_{ij}]$$

then

$$A_s = [R_{ij} a_{ij}]$$

in which

$$R_{ij} = X_j / X_i \tag{2.9}$$

Thus the actual ratios of scale factors are of predominant importance for scaling the system matrix, and the scaling problem centers around the selection of that set of ratios. Assigning scaling factors as outlined by Brockus, we present a typical A and A_s (scaled) in Table 1. The conditioning of these two arrays is significantly different with A_s several orders of magnitude better than the original unscaled array A. The B matrix was also scaled to B_s with a "1" for the single input element, fuel flow, and a "0" for all others.

2.2 State Feedback Control. To implement a full-state feedback law of the form [7]

$$u = -g^T \mathbf{x} \tag{2.10}$$

where g is $(n \times l)$, the "place" command in MATLAB using Ackerman's formula was exercised. Fuel flow, u, is the single input for this system.

Three operating points (100, 50, and 0 percent load) were examined in detail. Eigenvalues of the identified A matrices from ACSL each had one right half-plane pole. We arbitrarily elected to move the poles to stable points in the s plane, solve for the q_i's and then do a linear system simulation about the designated operating point. Further, to perturb the system the speed (XNH) was varied by 5 percent for each operating point. Table 2 contains a typical set of eigenvalues for A_s and $A_s - Bg^T$.

Once the feedback gains have been obtained, a simulation over a 10 second interval using the load transient depicted in Fig. 2 was run in ACSL and the results are shown in Fig. 3. There are, of course, an infinite number of possibilities for the selection of the eigenvalues.

2.3 Linear Quadratic Regulator (LQR) Control. The solution of the LQR control problem [7] amounts to calculating the optimal feedback gain matrix K such that the feedback law

$$u = -K \mathbf{x} \tag{2.11}$$

A:

$$\begin{bmatrix} -8.1e-1 & 0 & -2.9e-1 & -1.4e4 & 6.9e-1 & 2.6e3 & -9.9e-2 & -2.1e2 \\ 1 & 0 & 0 & 0 & 0 & 0 & 0 & 0 \\ -2.8e1 & 0 & -3.8e3 & -1.4e8 & 1.05e3 & 7.1e5 & -2.8e2 & -6.3e5 \\ -3.1e-4 & 0 & -1.4e-1 & -8.3e3 & 8.1e-3 & 8.0e1 & -2.7e-3 & -5.5 \\ 1.9 & 0 & 6.0e-1 & 1.1e4 & 2.1e2 & 1.9e6 & -6.2e2 & -1.5e6 \\ 1.05e-3 & 0 & 3.4e-4 & 6.2 & -1.7e-1 & -9.6e2 & 3.6e-1 & 7.9e2 \\ 4.5e1 & 0 & 0 & 0 & 1.3e2 & 7.1e5 & -3.6e2 & -6.0e5 \\ 3.9e-2 & 0 & 0 & 0 & 1.6e-1 & 8.8e2 & -3.6e-1 & -7.9e2 \end{bmatrix}$$

A_ς :

$$\begin{bmatrix} -8.1e-1 & 0 & -2.9e1 & -4.3e1 & 2.2 & 2.6 & -1.4e-1 & -2.2e-1 \\ 1.1 & 0 & 0 & 0 & 0 & 0 & 0 & 0 \\ -2.8e-1 & 0 & -3.8e3 & -4.4e3 & 3.4e1 & 6.9 & -3.7 & -6.5 \\ -9.8e-2 & 0 & -4.4e3 & -8.3e3 & 8.3 & 2.5e1 & -1.1 & -1.8 \\ 5.8e-1 & 0 & 1.9e1 & 1.1e1 & 2.1e2 & 5.7e2 & -2.6e2 & -5.0e2 \\ 1.1 & 0 & 3.5e1 & 2.0e1 & -5.5e2 & -9.6e2 & 5.0e2 & 8.4e2 \\ 3.3e1 & 0 & 0 & 0 & 3.0e2 & 5.1e2 & -3.6e2 & -4.5e2 \\ 3.8e1 & 0 & 0 & 0 & 4.9e2 & 8.3e2 & -4.8e2 & -7.9e2 \end{bmatrix}$$

Table 2 Eigenvalues

A_ς	$A_\varsigma - Bg^T$
-1.0976e+04	-1.0976e+04
-1.6660e+03	-1.6660e+03
-1.1471e+03	-1.1471e+03
-1.2181e+02	-1.2181e+02
4.8941e-01	-7.2998e+01
-7.2998e+01	-5.0000e-01
-4.0995e+01	-4.0995e+01

minimizes the cost function

$$J = \int_0^{tf} (\mathbf{x}\, Q\mathbf{x} + \mathbf{u}\, R\mathbf{u})\, dt \qquad (2.12)$$

subject to the constraint equation

$$\mathbf{x} = A\mathbf{x} + B\mathbf{u} \qquad (2.13)$$

Assuming the A and B arrays identified in ACSL for the different operating points are correct, then the main difficulty is selecting Q and R subject to the further constraints that Q be symmetric and positive semidefinite and the R be symmetric and positive definite.

Since only one input (fuel flow) is in the model, R may be any positive number. Once again, the choices and possibilities are endless. So for the purpose of getting started Q was chosen to be the $(n \times n)$ identity array and R was chosen to be "1" for the first case. The gains K were found using MATLAB at all three operating points and a simulation using one of these results was done over the standard load transient shown in Fig. 2. The results, shown in Fig. 4, show the LQR determined controller to compare favorably with the commercial analog controller.

2.4 Bellman Solution for Optimization. Given a homogeneous state equation

$$\dot{\mathbf{x}} = A\mathbf{x} \qquad (2.14)$$

with quadratic cost function of the form

$$J = \int_0^\infty \mathbf{x}\, R\mathbf{x}\, dt \qquad (2.15)$$

then the Bellman solution uses the Lyapunov function

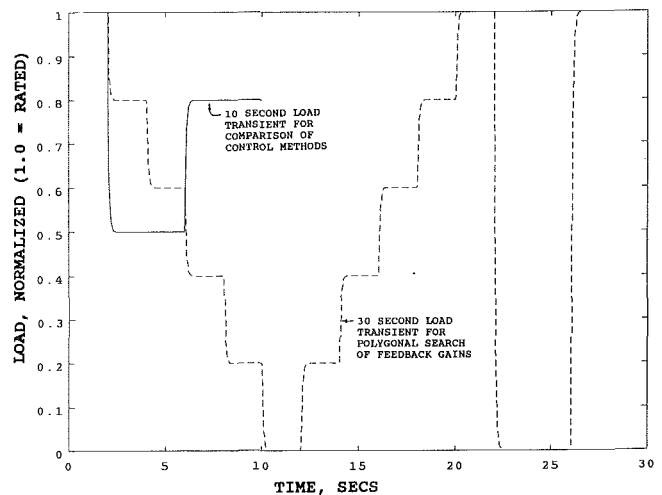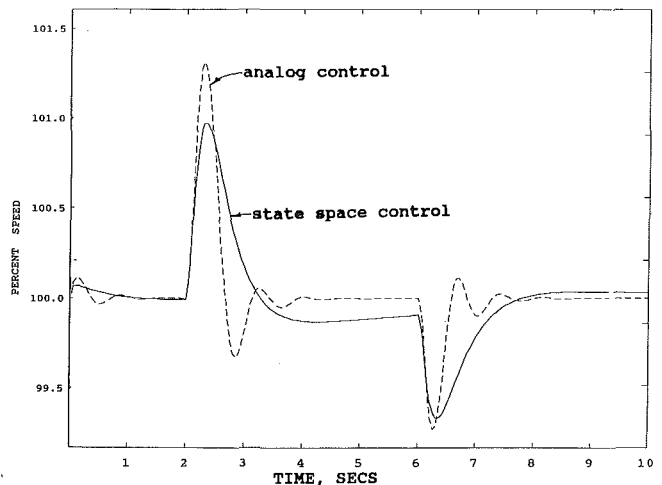$$R = A^T F + F A \qquad (2.16)$$

Fig. 2 Load transients

Fig. 3 Comparison of state feedback controller with analog controller

with F a symmetric matrix. Find F to minimize the cost function

$$J = -\mathbf{x}^T(0) F \mathbf{x}(0) \qquad (2.17)$$

Our linearized control system with control law $u = -k\mathbf{x}$ is just the form for the Bellman optimization. The gains K are perturbed to minimize the cost function (Eq. (2.17)). Simulation results for this optimization scheme are given in Fig. 5. Figure
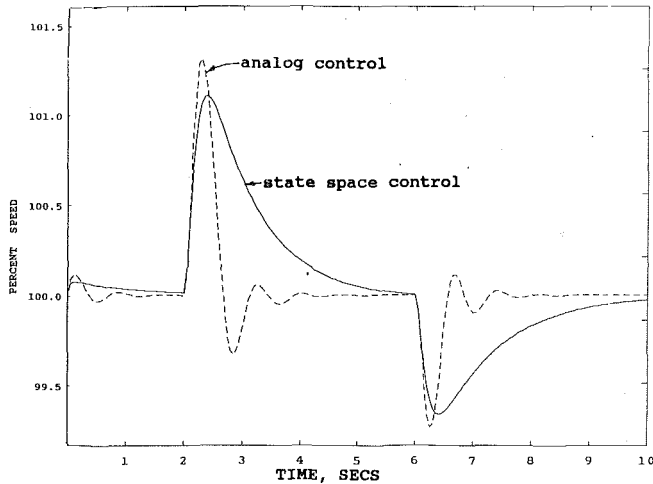
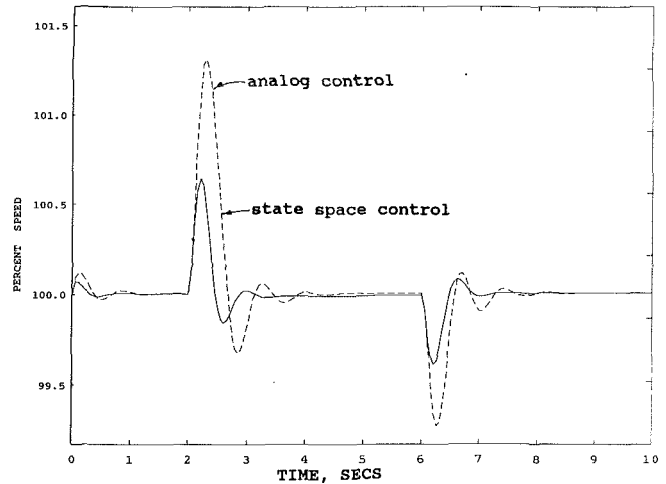Fig. 4 Comparison of LQR feedback controller with analog controller

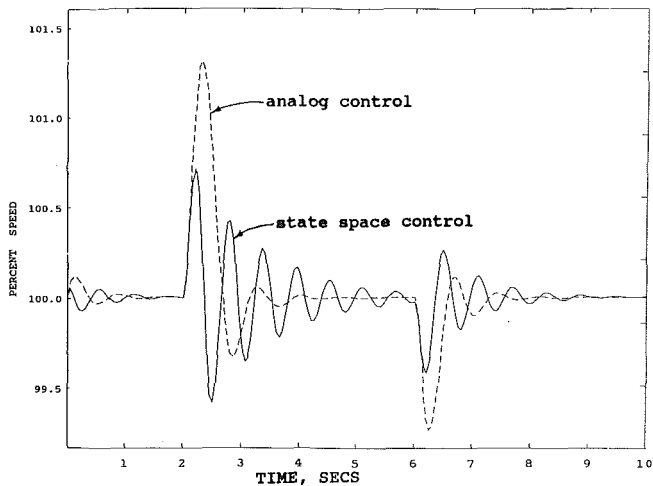Fig. 6 Comparison of Bellman feedback controller with analog controller (with presetting)

Fig. 5 Comparison of Bellman feedback controller with analog controller (no presetting)

Fig. 7 Comparison of polygonal search feedback controller with analog controller (no speed sensing delay)

6 is an improvement over the results shown in Fig. 5 and required presetting some of the eigenvalues.

2.5 Polygonal Search. One method of obtaining fuel control feedback gains is through a search optimization technique as follows:

1 The parameters in the search are the feedback gains.
2 The cost function is the integral of the speed error over some arbitrary load transient.
3 The "optimal" gains are obtained by repeated runs of the simulation over the arbitrary load transient.

A flexible polygonal search [8] works well in this case. The parameters (up to nine in number) create a search polygon in nine space that becomes oblong in the direction of cost function improvement as the search progresses. Figure 2 shows the somewhat extravagant 30 second load transient that was used for this method. A lot of computer time is required for this method so batch run were made overnight. The various sets of feedback gains and the resultant eigenvalues are shown in Table 3. Figure 7 is a comparison of the fuel control using gains obtained by the polygonal search versus the analog fuel control where it is noted that the state feedback gains control extremely well. Part of this is because the delay in speed sensing was removed for this initial search. When the sensing delay was put back into the model the transient curve shown in Fig. 8 was obtained. It still does much better than the analog control, but a lead circuit (anticipatory) can be applied to the
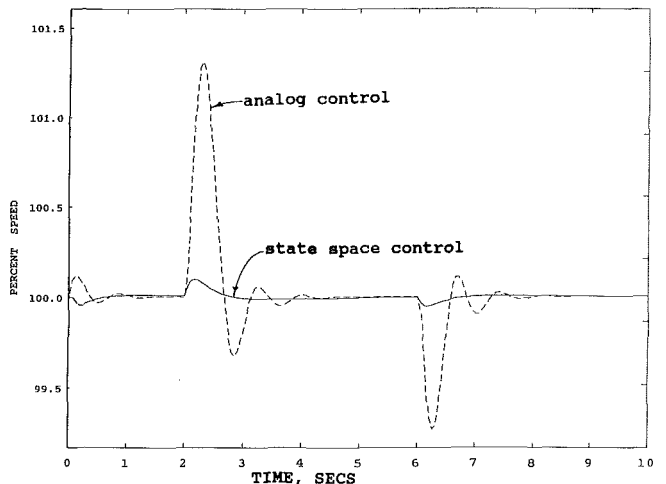
speed sensing and reduce the effect of the sensing delay. Figure 9 shows the transient with this lead circuit present. An interesting result is shown in Fig. 10. The feedback gains for this control are also presented in Table 3 where it can be noted that only three states were used in the control. The polygonal search was thus only a search in three space. The extremely tight control is probably not realizable in practice because of the very high gain on the derivative of speed, which as noted before, is too subject to noise to be practical.

3.0 Summary and Conclusions

Several different schemes for arriving at controllers for a gas turbine engine have been investigated. An analog model programmed in ACSL was used to develop a linearized state-space representation for use in MATLAB. The different approaches for obtaining feedback gains and the results from each set of gains are presented. The approaches are: state feedback, LQR, Bellman, and polygonal search.

The state-space approach to developing controllers is a viable one for simulations of this size and larger. In particular, multi-input, multimode fuel controllers are readily adaptable to this approach.

No comparison has been attempted to analyze which of these state-space approaches is the "best" other than a graphical

Table 3 Feedback gains and eigenvalues

Feedback Gains:

Fig 3	Fig 4	Fig 5	Fig 6	Fig 7	Fig 8	Fig 9	Fig10
-7.442	-3.497	-60.36	-41.26	-61.10	-61.25	-62.37	-3945.
-1.924	-.0470	-1.398	-4.683	-159.4	-157.3	-156.9	143.9
.00025	.00012	.00026	0	56.40	58.34	58.54	0
7.920	3.991	6.248	0	16.00	18.87	20.46	0
.0255	-.0130	-.6e-6	0	-14.00	-9.464	-2.180	0
-278.2	-141.0	-9016.	0	-150.0	-146.6	-139.8	0
-.0257	-.0129	-.0124	0	-340.7	-336.9	-336.9	0
-207.7	-105.4	-37.36	0	-430.0	-428.9	-427.1	0

Derivative of Speed feedback gain:

0	0	0	0	-100.0	-97.93	-97.56	-3436.

Eigenvalues (of A+B*K):

| Fig 3	Fig 4	Fig 5	Fig 6	Fig 7	Fig 8	Fig 9	Fig10
-10976	-10976	-10976.	-10976	-11938	-11872	-11799	-18576
-1667.	-1666.	-1737.6	-1666.	-5723.	-5363.	-4909.	-10366
-1147.	-1147.	-1146.8	-1147.	-2123.	-2140.	-2151.	-1370.
-116.4	-121.9	-23.6+j35.4	-101.5	-615.2	-559.9	-492.4	-1051.
-73.51	-72.97	-23.6-j35.4	-80.86	-33.39	-31.16	-26.10	-1.182
-.4730	-40.99	-72.66	-10.52	-.9627	-.7840	-5.360	-354.2
-1.098	-.4191	-44.04	-.1204	-1.958	-54.94	-.6863	-37.74
-41.03	-.0291	-.0219	-42.69	-56.41	-3.053	-52.93	-65.29
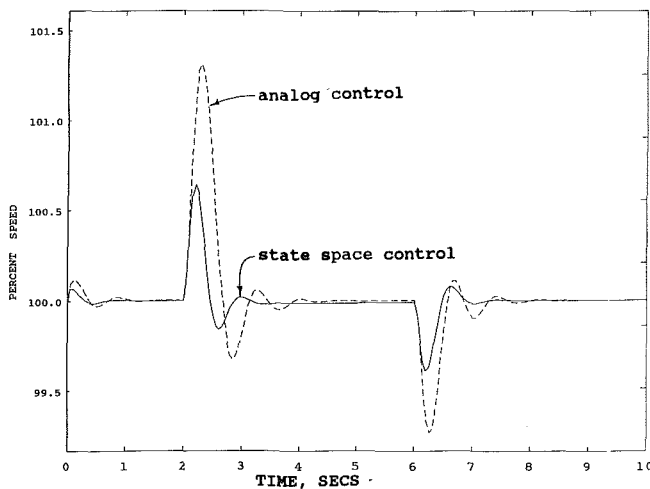
Fig. 8 Comparison of polygonal search feedback controller with analog controller (with speed sensing delay)
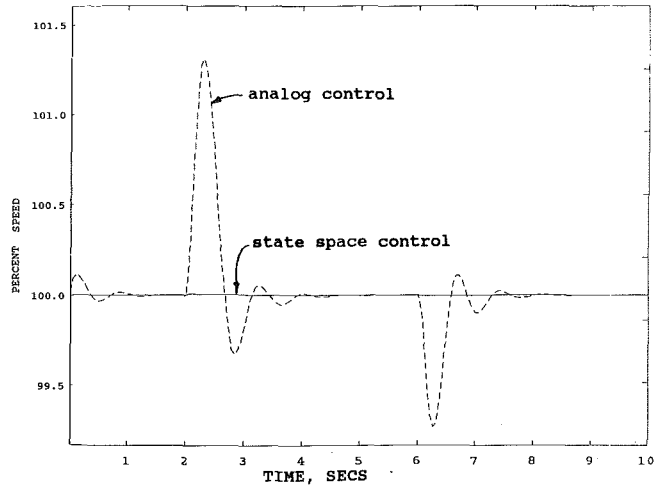

Fig. 10 Comparison of polygonal search (three states) feedback controller with analog controller
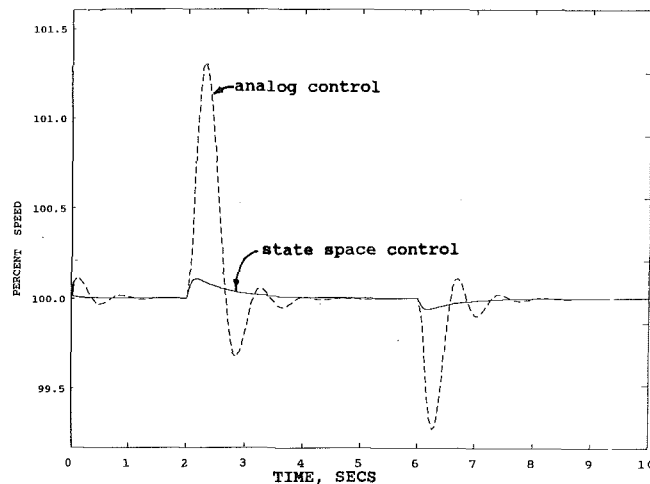

Fig. 9 Comparison of polygonal search feedback controller with analog controller (with lead filter)

comparison of the controller in action. Much research of the seemingly endless variations in these methods needs to be conducted.

References

1 Harmon, R. A., "Marine Gas Turbines: A New Generation," *Mechanical Engineering*, May 1990, pp. 48-51.

2 Mitchell and Gathier Associates, *Advanced Continuous Simulation Language Reference Manual*, 1986.

3 Daniels, C. J., et al., "Digital Computer Program for Generating Dynamic Turbofan Engine Models (DIGTEM)," NASA Technical Memorandum 83446, Sept. 1983.

4 Phillips, C. L., and Harbor, R. D., *Feedback Control Systems*, Prentice-Hall, 1988.

5 PRO-MATLAB, the Mathworks, 1987.

6 Brockus, C. G., "Scaling the Equations for Polynomial Least Mean Squares Curve Fitting," *Proceedings of the 19th Annual Pittsburgh Modeling and Simulation Conference*, Vol. 19, Part 5, pp. 2077-2081.

7 D'Azzo, J. J., and Houpis, C. H., *Linear Control System Analysis and Design*, 3rd ed., McGraw-Hill, New York, 1988.

8 Himmelblau, D. M., *Applied Nonlinear Programming*, McGraw-Hill, New York, 1972.